

Recommendation ITU-R P.2040-4 (09/2025)

P Series: Radio-wave propagation

Effects of building materials and structures on radio-wave propagation in the range of 1 MHz to 450 GHz



Foreword

The role of the Radiocommunication Sector is to ensure the rational, equitable, efficient and economical use of the radio-frequency spectrum by all radiocommunication services, including satellite services, and carry out studies without limit of frequency range on the basis of which Recommendations are adopted.

The regulatory and policy functions of the Radiocommunication Sector are performed by World and Regional Radiocommunication Conferences and Radiocommunication Assemblies supported by Study Groups.

Policy on Intellectual Property Right (IPR)

ITU-R policy on IPR is described in the Common Patent Policy for ITU-T/ITU-R/ISO/IEC referenced in Resolution ITU-R 1. Forms to be used for the submission of patent statements and licensing declarations by patent holders are available from https://www.itu.int/ITU-R/go/patents/en where the Guidelines for Implementation of the Common Patent Policy for ITU-T/ITU-R/ISO/IEC and the ITU-R patent information database can also be found.

Series of ITU-R Recommendations								
	(Also available online at https://www.itu.int/publ/R-REC/en)							
Series	Title							
ВО	Satellite delivery							
BR	Recording for production, archival and play-out; film for television							
BS	Broadcasting service (sound)							
BT	Broadcasting service (television)							
F	Fixed service							
M	Mobile, radiodetermination, amateur and related satellite services							
P	Radio-wave propagation							
RA	Radio astronomy							
RS	Remote sensing systems							
\mathbf{S}	Fixed-satellite service							
SA	Space applications and meteorology							
SF	Frequency sharing and coordination between fixed-satellite and fixed service systems							
SM	Spectrum management							
SNG	Satellite news gathering							
TF	Time signals and frequency standards emissions							
V	Vocabulary and related subjects							

Note: This ITU-R Recommendation was approved in English under the procedure detailed in Resolution ITU-R 1.

Electronic Publication Geneva, 2025

© ITU 2025

All rights reserved. No part of this publication may be reproduced, by any means whatsoever, without written permission of ITU.

RECOMMENDATION ITU-R P.2040-4

Effects of building materials and structures on radio-wave propagation in the range of 1 MHz to 450 GHz

(Question ITU-R 211/3)

(2013-2015-2021-2023-2025)

Scope

This Recommendation provides guidance on the effects of building materials and structures on radio-wave propagation in the range of 1 MHz to 450 GHz.

Keywords

Permittivity, permeability, conductivity, wave impedance, building materials, reflection coefficients, transmission coefficients

Related ITU Recommendations and Reports

Recommendation ITU-R P.526 – Propagation by diffraction

Recommendation ITU-R P.527 – Electrical characteristics of the surface of the Earth

Recommendation ITU-R P.679 – Propagation data required for the design of broadcasting-satellite systems

Recommendation ITU-R P.1238 – Propagation data and prediction methods for the planning of indoor radiocommunication systems and radio local area networks in the frequency range 300 MHz to 450 GHz

Recommendation ITU-R P.1406 – Propagation effects relating to terrestrial land mobile and broadcasting services in the VHF and UHF bands

Recommendation ITU-R P.1407 – Multipath propagation and parameterization of its characteristics

Recommendation ITU-R P.1411 – Propagation data and prediction methods for the planning of short-range outdoor radiocommunication systems and radio local area networks in the frequency range 300 MHz to 100 GHz

Recommendation ITU-R P.1812 – A path-specific propagation prediction method for point-to-area terrestrial services in the frequency range 30 MHz to 6 GHz

Report ITU-R P.2346 – Compilation of measurement data relating to building entry loss

NOTE – The latest edition of the Recommendation/Report in force should be used.

The ITU Radiocommunication Assembly,

considering

- a) that electrical properties of materials and their structures strongly affect radio-wave propagation;
- b) that it is necessary to understand the losses of radio-waves caused by building materials and structures;
- c) that there is a need to give guidance to engineers to avoid interference from outdoor to indoor and indoor to outdoor systems;
- d) that there is a need to provide users with a unified source for computing effects of building materials and structures,

noting

- a) that Recommendation ITU-R P.526 provides guidance on diffraction effects, including those due to building materials and structures;
- b) that Recommendation ITU-R P.527 provides information on the electrical properties of the surface of the Earth;
- c) that Recommendation ITU-R P.679 provides guidance on planning broadcasting-satellite systems;
- d) that Recommendation ITU-R P.1238 provides guidance on indoor propagation over the frequency range 900 MHz to 100 GHz;
- e) that Recommendation ITU-R P.1406 provides information on various aspects of propagation relating to terrestrial land mobile and broadcasting services in the VHF and UHF bands;
- f) that Recommendation ITU-R P.1407 provides information on various aspects of multi-path propagation;
- g) that Recommendation ITU-R P.1411 provides propagation methods for short paths in outdoor situations, in the frequency range from about 300 MHz to 100 GHz;
- h) that Recommendation ITU-R P.1812 provides a propagation prediction method for terrestrial point-to-area services in the frequency range 30 MHz to 6 GHz,

recommends

that the information and methods in the Annex should be used as a guide for the assessment of the effects of building material properties and structures on radio-wave propagation, and in developing deterministic models of propagation involving the built environment.

The Annex describes basic principles, and provides expressions to evaluate reflection from and transmission through building materials and structures. It also includes a model for electrical properties as a function of frequency, and a table of parameters for relevant materials.

Examples of building-entry loss measurements may be found in Report ITU-R P.2346.

Annex

TABLE OF CONTENTS

D

				ruge
Poli	ey on I	ntellectua	l Property Right (IPR)	ii
Ann	ex	•••••		2
1	Introd	duction		3
2	Basic	principle	s and theory	3
	2.1	Theory	of material electrical properties	3
		2.1.1	Introduction	3
		2.1.2	Method	4
		213	Frequency dependence of material properties	9

		2.1.4	Models of material properties frequency dependence	9
	2.2	Effects	of material structure on radio-wave propagation	9
		2.2.1	Plane wave reflection and transmission at a single planar interface	9
		2.2.2	Plane wave reflection and transmission for a single- or multi-layer slab	14
		2.2.3	Waveguide propagation in buildings	18
	2.3	Theory	and results for frequency selective surface materials	21
		2.3.1	Frequency selective surfaces	21
		2.3.2	Theory for wave propagation around the surface of round convexity array	22
		2.3.3	Calculation results	23
		2.3.4	Measurement	24
3	Comp	oilations o	of electrical properties of materials	24
Atta	coeffi	cients fo	nnex 1 Alternative method to obtain reflection and transmission or building materials represented by N dielectric slabs based on ABCD atton.	27

1 Introduction

This Annex provides guidance on the effects of building material electrical properties and structures on radio-wave propagation.

Section 2 describes fundamental principles concerning the interaction of radio waves with building materials, defines various parameters in use for these purposes, and gives basic expressions for reflection from and transmission through single material interfaces and single and multiple layer slabs, typical of building construction.

Section 3 defines a model for electrical properties, and a table of parameters for various building materials.

2 Basic principles and theory

Radio waves that interact with a building will produce losses that depend on the electrical properties of the building materials and material structure. In this section, theoretical effects of material electrical properties and structure on radio-wave propagation will be discussed.

2.1 Theory of material electrical properties

2.1.1 Introduction

This section describes the development of simple frequency-dependent formulae for the permittivity and conductivity of common building materials. The formulae are based on curve fitting to a number of published measurement results, mainly in the frequency range 1-100 GHz. The aim is to find a simple parameterization for use in indoor-outdoor ray trace modelling.

The characterization of the electrical properties of materials is presented in a number of different ways in the literature. These are described in § 2.1.2 in order that the measured data can be reduced to a common format.

2.1.2 Method

2.1.2.1 Definitions of electrical constants

The following treatment deals only with non-ionized, non-magnetic materials, and throughout we therefore set the free charge density, ρ_f , to zero and the permeability of the material, μ , to the permeability of free space μ_0 .

The fundamental quantities of interest are the electrical permittivity, ε , and the conductivity, σ . There are many ways of quantifying these parameters in the literature, so we first make explicit these different representations and the relations between them.

2.1.2.2 Derivation

The starting point is the wave equation derived from Maxwell's equations. Under the above assumptions, the wave equation for the electric field \vec{E} is:

$$\nabla^2 \vec{E} - \varepsilon \mu_0 \frac{\partial^2 \vec{E}}{\partial t^2} = \mu_0 \frac{\partial \vec{J}f}{\partial t} \tag{1}$$

where:

 \vec{E} : (vector) electric field intensity (V/m)

 J_f : current density of free charges (A/m²)

ε: dielectric permittivity (F/m)

 μ_0 : permeability of free space $(N/A^2) = 4\pi \times 10^{-7}$ by definition.

In a conductor, \vec{J}_f is related to \vec{E} through Ohm's Law by:

$$\vec{J}_f = \sigma \vec{E} \tag{2}$$

where:

 σ : conductivity (S/m).

Combining equations (1) and (2) gives:

$$\nabla^2 \vec{E} - \varepsilon \mu_0 \frac{\partial^2 \vec{E}}{\partial t^2} = \mu_0 \sigma \frac{\partial \vec{E}}{\partial t} \tag{3}$$

Writing \vec{E} in exponential notation:

$$\vec{E} = \vec{E}_0 e^{j(\omega t - \vec{k} \cdot \vec{r})} \tag{4}$$

where:

 \vec{E}_0 : value of \vec{E} for $t = \vec{r} = 0$ (V/m)

 \vec{k} : (vector) wave number (m⁻¹) magnitude = $2\pi/\lambda$ where λ is the wavelength in m

 ω : angular frequency (s⁻¹) = $2\pi f$ where f is the frequency in s⁻¹

 \vec{r} : (vector) spatial distance (m).

From equations (3) and (4) the following is obtained:

$$\nabla^2 E = j\omega\mu_0(\sigma + j\omega\varepsilon)\vec{E} \tag{5}$$

Equation (5) shows that the electric field propagates as an attenuated sinusoidal wave.

It is important to distinguish two situations of application according to the type of propagation medium, as described below.

2.1.2.3 Lossless dielectric (non-conductive)

In a lossless dielectric, the field is unattenuated. From equation (5), with $\sigma = 0$, the following results:

$$\nabla^2 E = j\omega\mu_0(j\omega\varepsilon)\bar{E} \tag{6}$$

For a plane wave propagating in the direction of the z-axis, the field is:

$$\bar{E} = E_{x}(z) \cdot \hat{x}$$

where \hat{x} is the unit vector in the direction of the x-axis.

Applying equation (5), it follows:

$$\frac{\partial^2 E_x}{\partial z^2} + \omega^2 \mu \varepsilon E_x = 0$$

The general solution of this equation is:

$$E_{x}(z) = E_{0}^{+} \cdot e^{-jkz} + E_{0}^{-} \cdot e^{jkz}$$

The first term represents the so-called progressive wave and the second the regressive wave; k is the wave number or propagation constant, whose value is:

$$k = \omega \sqrt{\mu \epsilon}$$
 (rad/m)

From it the phase velocity or velocity of propagation is deduced:

$$v_p = \frac{\omega}{k} = \frac{1}{\sqrt{\mu \varepsilon}}$$
 (m/s)

The relative dielectric permittivity of medium ε_r is defined as:

$$E_r = \frac{\varepsilon}{\varepsilon_o} \tag{7}$$

 ε_o being the dielectric permittivity of free space ($\varepsilon_o = 8.854 \times 10^{12} \left(\frac{F}{m}\right)$).

For non-magnetic medium, $\mu = \mu_o \left(4\pi \times \frac{10^{-7}H}{m} \right)$, so, in free space:

$$v_p = c = \frac{1}{\sqrt{\mu_o \varepsilon_o}}$$

where c is the speed of propagation of light in free space $\left(c = 299792.46 \times 10^3 \frac{\text{m}}{\text{s}}\right)$.

Combining the previous expressions, the phase velocity in a non-conducting medium of relative dielectric permittivity ε_r , is obtained:

$$v_p = \frac{c}{\sqrt{\varepsilon_r}} \tag{8}$$

The magnitude $\sqrt{\varepsilon_r}$, is called the refractive index of the dielectric medium.

2.1.2.4 Conducting dielectric

When $\sigma \neq 0$, the wave attenuates as it propagates. Equation (5) must be used to describe this propagation.

If equations (5) and (6) are compared, it can be seen that they are similar if a complex dielectric permittivity ε_c , is defined such that:

$$j\omega\varepsilon_c = \sigma + j\omega\varepsilon$$

or

$$\varepsilon_c = \varepsilon - j \frac{\sigma}{\omega} \tag{9}$$

and the developments of the previous case can be employed using ε_c which, referring to the free space dielectric permittivity ε_o , is expressed as the complex relative dielectric permittivity $\varepsilon_{rc} = \frac{\varepsilon_c}{\varepsilon_o}$.

Now, the wavenumber (vector) is complex:

$$k = j\omega\sqrt{\mu\varepsilon_c} = \alpha + j\beta$$

where α is the attenuation constant and β is the phase constant.

The values of α and β are:

$$A = \omega \sqrt{\frac{\mu \epsilon}{2} \left[\sqrt{1 + \left(\frac{\sigma}{\omega \epsilon}\right)^2} - 1 \right]} \quad (Np/m)$$

$$B = \omega \sqrt{\frac{\mu \epsilon}{2} \left[\sqrt{1 + \left(\frac{\sigma}{\omega \epsilon} \right)^2} + 1 \right]} \quad (rad/m)$$

The phase velocity is:

$$v_p = \frac{\omega}{\beta}$$

In electromagnetics texts in general and in Recommendation ITU-R P.527-5, ε_{rc} is expressed as:

$$\varepsilon_{rc} = \varepsilon_r' - j\varepsilon_r'' = \frac{\varepsilon}{\varepsilon_o} - \frac{j\sigma}{\omega\varepsilon_o}$$
 (10)

The imaginary part of ε_{rc} is:

$$\varepsilon_r^{\prime\prime} = \frac{\sigma}{\omega \varepsilon_0} \tag{11}$$

Note that the sign of the imaginary part of ε_{rc} is arbitrary and reflects the sign convention in equation (4). In practical units, equation (12) performs a conversion from ε_r'' to σ :

$$\sigma = 0.05563 \,\varepsilon_r'' f_{\text{GHz}} \tag{12}$$

Another formulation of the imaginary part of η is in terms of the loss tangent, defined as:

$$\tan \delta = \frac{\varepsilon_r''}{\varepsilon_r'} \tag{13}$$

and so:

$$\tan \delta = \frac{\sigma}{\omega \varepsilon} \tag{14}$$

From equation (10) this gives:

$$\varepsilon_{rc} = \varepsilon_r' (1 - j \tan \delta) \tag{15}$$

and in practical units:

$$\sigma = 0.05563 \,\varepsilon_r' \tan \delta \, f_{\rm GHz} \tag{16}$$

Another term sometimes encountered is the Q of the medium. This is defined as:

$$Q = \frac{\varepsilon \omega}{\sigma} \tag{17}$$

and is the ratio of the displacement current density $\partial D/\partial t$ to the conduction current density J_f . For non-conductors, $Q \to \infty$. From equation (14):

$$Q = 1/\tan \delta \tag{18}$$

Yet another term encountered is the complex refractive index n which is defined as $\sqrt{\varepsilon_{rc}}$. Writing n in terms of its real and imaginary parts:

$$n = n' - jn'' = \sqrt{\varepsilon_{rc}} \tag{19}$$

n', n'' and σ are obtained from equations (10) and (12):

$$\varepsilon'_r = (n')^2 - (n'')^2$$

$$\varepsilon_r'' = 2n'n''$$

$$\sigma = 0.1113 n'n'' f_{\text{GHz}}$$
(20)

2.1.2.5 Attenuation rate

A conducting dielectric will attenuate electromagnetic waves as they propagate. To quantify this, substitute equation (5) in equation (4) and simplify using equation (14):

$$\vec{E} = \vec{E}_0 \exp\{j(\omega t - \sqrt{\varepsilon'(1 - j \tan \delta)} \vec{k}_0 \cdot \vec{r})\}$$
(21)

where:

 \vec{k}_0 : (vector) wave number (m⁻¹) in free space.

The imaginary part under the square root sign leads to an exponential decrease of the electric field with distance:

$$\vec{E} \propto \vec{E}_0 \exp(-|\vec{r}|/\Delta)$$
 (22)

In a practical calculation using complex variables, the attenuation distance, Δ , at which the field amplitude falls by 1/e, can be evaluated as:

$$\Delta = \frac{-1}{\operatorname{Im}(k_0 \sqrt{\varepsilon})} \tag{23a}$$

where the function "Im" returns the imaginary part of its argument. Analytically it can be shown that:

$$\Delta = \frac{1}{k_0 \sqrt{\eta'}} \sqrt{\frac{2 \cos \delta}{1 - \cos \delta}} \tag{23b}$$

which can be evaluated by calculating $\tan \delta$ from ϵ' and σ and inverting to obtain $\cos \delta$. More direct evaluation is possible in the two limits of $\sigma \to 0$ (dielectric limit) and $\sigma \to \infty$ (good conductor limit). By choosing the appropriate approximation of the term under the square root sign in equation (21) these limits are:

$$\Delta_{dielectric} = \frac{1}{k_0 \sqrt{\varepsilon'}} \frac{2}{\tan \delta}$$
 (24)

and:

$$\Delta_{conductor} = \frac{1}{k_0 \sqrt{\varepsilon'}} \sqrt{\frac{2}{\tan \delta}}$$
 (25)

Equations (24) and (25) are accurate to about 3% for tan δ < 0.5 (dielectric) tan δ > 15 (conductor). $\Delta_{conductor}$ is usually referred to as the "skin depth".

For practical purposes the attenuation rate is a more useful quantity than the attenuation distance, and is related to it simply by

$$A = \frac{20\log_{10}e}{\Delta} = 8.686/\Delta \tag{26}$$

where:

A: attenuation rate in dB/m (with Δ in m).

Substituting equations (24) and (25) in equation (26) and converting to practical units gives:

$$A_{dielectric} = 1 636 \frac{\sigma}{\sqrt{\varepsilon'}}$$
 (27a)

$$A_{conductor} = 545.8\sqrt{\sigma f_{\text{GHz}}} \tag{27b}$$

2.1.3 Frequency dependence of material properties

In the literature, the real part of the dielectric constant, ε' , is always given, but often the frequency is not specified. In practice for many materials, the value of ε' is constant from DC up to around 5-10 GHz after which it begins to fall with frequency.

The value of σ is usually a strong function of frequency in the band of interest, increasing with frequency. This may be one reason why the imaginary part of the dielectric constant, or the loss tangent, is often specified in the literature: equations (12) and (16) show that these terms remove a linear frequency dependence compared to the frequency dependence of σ .

For each material a simple regression model for the frequency dependence of σ can be obtained by fitting to measured values of σ at a number of frequencies.

2.1.4 Models of material properties frequency dependence

In order to derive the frequency dependence of material properties, the values of the electrical constants of the materials can be characterized in terms of the measurement frequency, real part (ϵ ') and imaginary part (ϵ '') of the relative permittivity, loss tangent ($\tan \delta$) and conductivity (σ). Expressions in § 2.1.2.4 permit conversions between these quantities.

For the conductivity, there is usually statistically significant evidence for an increase with frequency. In this case the trend has been modelled using:

$$\sigma = c f_{\text{GHz}}^d \tag{28}$$

where c and d are constants characterizing the material. This is a straight line on a $\log(\sigma)$ – $\log(f)$ graph. The trend line is the best fit to all available data.

For the relative permittivity one can assume similar frequency dependency:

$$\varepsilon' = a f_{\text{GHz}}^b \tag{29}$$

where a and b are constants characterizing the material. However, in almost all cases there is no evidence of a trend of relative permittivity with frequency. In these cases, a constant value can be used at all frequencies. The constant value is the mean of all the values plotted. Some examples are given in Table 3.

2.2 Effects of material structure on radio-wave propagation

2.2.1 Plane wave reflection and transmission at a single planar interface

This section considers a plane wave incident upon a planar interface between two homogeneous and isotropic media of differing electric properties. The media extend sufficiently far from the interface such that the effect of any other interface is negligible. This may not be the case with typical building geometries. For example, propagation losses due to a wall may be influenced by multiple internal

reflections. Methods for calculating reflection and transmission coefficients of single-layer and multilayer slabs are given in § 2.2.2.

A plane wave is useful for analysis purposes, but the concept is largely theoretical. In practice a wave may approximate but not be exactly planar. The point is important here because a truly plane wave does not experience free-space (spreading) loss. The following methods take no account of free-space losses, only the effect of the media interface.

2.2.1.1 Oblique incidence on a plane media interface

Figure 1 illustrates a sinusoidal plane wave incident obliquely to a plane interface separating two uniform non-magnetic dielectric media with relative permittivities are ε_{r1} and ε_{r2} . The values of ε_r can be calculated from the real part of the relative permittivity ε_r' and the conductivity σ , using equations (10) and (11). Table 3 provides parameters from which these can be calculated as functions of frequency. It is important to clarify that when one or both media have losses the oblique incidence problem does not admit as a solution a superposition of homogeneous plane waves. In these cases, the direction of propagation depends, in general, on the amplitudes of the fields and an interpretation of Snell's laws is not possible independently of them. However, the reflected wave is of the same type (homogeneous or not) as the incident wave, regardless of the characteristics of the media.

There are three important theorems for this case that follow from geometrical considerations.

- 1) The vector wave numbers of the reflected and transmitted (refracted) waves lie in the plane of incidence, i.e. the plane defined by wave number k_i of the incident wave and the normal to the interface. This is taken to be the x-z plane in Fig. 1.
- The angles of incidence and reflection are equal (both θ_1 in Fig. 1).
- The angle of refraction θ_2 is related to the angle of incidence θ_1 by Snell's law.

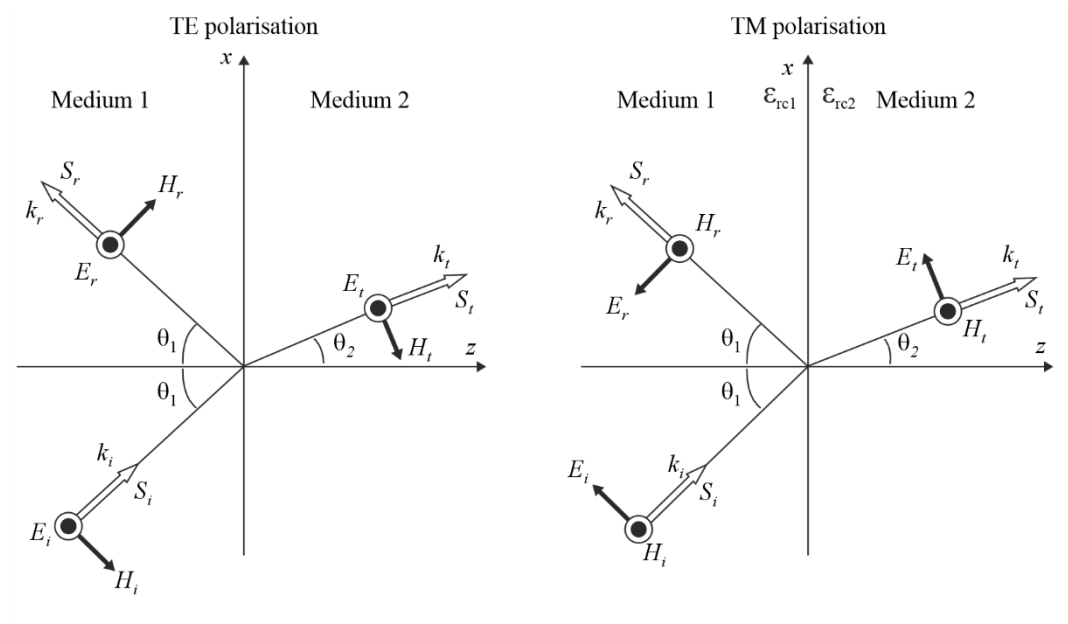
$$\sqrt{\varepsilon_{rc1}} \cdot \sin \theta_1 = \sqrt{\varepsilon_{rc2}} \cdot \sin \theta_2 \tag{30}$$

where ε_{rc1} and ε_{rc2} are the relative complex permittivities of media 1 and 2, respectively.

These theorems ensure that the exponential space-time factors, $\exp\{j(\omega t - k \cdot r)\}$, for the three waves $(k \to k_1, k_1, k_2, \text{respectively})$ are identical at all points in the interface.

FIGURE 1

Reflection and refraction of plane waves at plane interface



P.2040-01

Two polarizations of the incident wave are shown in Fig. 1.

- a) On the left the incident electric vector E_i is perpendicular to the plane of incidence. This is known as transverse electric (TE) polarisation. Other terms are perpendicular polarisation, s-polarisation, and σ -polarisation.
- b) On the right the incident electric vector E_i is parallel to the plane of incidence. This is known as transverse magnetic (TM) polarisation. Other terms are parallel polarisation, p-polarization, and π -polarization.

In the following descriptions, polarization will be designated by TE or TM.

An arbitrarily or circularly polarised wave can be resolved into its TE and TM components for calculation purposes, which can then be re-combined.

E-field reflection and transmission coefficients are defined as the ratios of reflected and transmitted (refracted) vectors respectively to the corresponding incident vector as they exist at the interface. In general such coefficients are complex. The following expressions take no account of free-space or other losses prior or subsequent to the interaction of a wave with the interface.

The requirement that electric and magnetic vectors are continuous in the plane of the interface give the following expressions for electric field coefficients. Reflection and transmission coefficients are denoted by R and T respectively. The subscripts indicate the vectors concerned, and whether the polarization is TE or TM. Each of equations (31a) to (32b) are in two parts, according to whether total internal reflection occurs. Total internal reflection is only possible when a wave is incident upon a medium with lower refractive index.

Equations (31a) to (32b) are only valid when the magnetic permeabilities of the two environments $(\mu_1; \mu_2)$ are equal to each other.

E-field reflection coefficient for TE polarisation:

$$R_{eTE} = \frac{E_r}{E_i} = \begin{cases} \frac{\sqrt{\varepsilon_{rc1}} \cos \theta_1 - \sqrt{\varepsilon_{rc2}} \cos \theta_2}{\sqrt{\varepsilon_{rc1}} \cos \theta_1 + \sqrt{\varepsilon_{rc2}} \cos \theta_2} & \sqrt{\left|\frac{\varepsilon_{rc1}}{\varepsilon_{rc2}}\right|} \sin \theta_1 < 1\\ 1 & \sqrt{\left|\frac{\varepsilon_{rc1}}{\varepsilon_{rc2}}\right|} \sin \theta_1 \ge 1 \end{cases}$$
(31a)

E-field reflection coefficient for TM polarisation:

$$R_{eTM} = \frac{E_r}{E_i} = \begin{cases} \frac{\sqrt{\varepsilon_{rc2}} \cos \theta_1 - \sqrt{\varepsilon_{rc1}} \cos \theta_2}{\sqrt{\varepsilon_{rc2}} \cos \theta_1 + \sqrt{\varepsilon_{rc1}} \cos \theta_2} & \sqrt{\frac{\varepsilon_{rc1}}{\varepsilon_{rc2}}} \sin \theta_1 < 1\\ 1 & \sqrt{\frac{\varepsilon_{rc1}}{\varepsilon_{rc2}}} \sin \theta_1 \ge 1 \end{cases}$$
(31b)

E-field transmission coefficient for TE polarisation:

$$T_{eTE} = \frac{E_t}{E_i} = \begin{cases} \frac{2\sqrt{\varepsilon_{rc1}}\cos\theta_1}{\sqrt{\varepsilon_{rc1}}\cos\theta_1 + \sqrt{\varepsilon_{rc2}}\cos\theta_2} & \sqrt{\left|\frac{\varepsilon_{rc1}}{\varepsilon_{rc2}}\right|}\sin\theta_1 < 1\\ 0 & \sqrt{\left|\frac{\varepsilon_{rc1}}{\varepsilon_{rc2}}\right|}\sin\theta_1 \ge 1 \end{cases}$$
(32a)

E-field transmission coefficient for TM polarisation:

$$T_{eTM} = \frac{E_t}{E_i} = \begin{cases} \frac{2\sqrt{\varepsilon_{rc1}}\cos\theta_1}{\sqrt{\varepsilon_{rc2}}\cos\theta_1 + \sqrt{\varepsilon_{rc1}}\cos\theta_2} & \sqrt{\left|\frac{\varepsilon_{rc1}}{\varepsilon_{rc2}}\right|}\sin\theta_1 < 1\\ 0 & \sqrt{\left|\frac{\varepsilon_{rc1}}{\varepsilon_{rc2}}\right|}\sin\theta_1 \ge 1 \end{cases}$$
(32b)

where ε_{rc1} and ε_{rc2} are the complex relative permittivities of medium 1 and 2 respectively. These can be evaluated using equation (9b) with values of η' and σ obtained from § 3 and Table 3.

The $\cos\theta_2$ terms in equations (31a) to (32b) can be evaluated in terms of θ_1 using equation (30) as:

$$\cos \theta_2 = \sqrt{1 - \frac{\varepsilon_{rc1}}{\varepsilon_{rc2}} \sin^2 \theta_1} \tag{33}$$

At $\theta_1 = 0$ the incidence plane is not uniquely defined. In this case all directions of propagation are normal to the interface, and the coefficient amplitudes from the expression for each polarisation is the same. In the case of reflection there is an apparent sign change. This arises purely from how the polarizations are defined; it is not a physical discontinuity.

2.2.1.2 Calculation examples

Figure 2 gives examples of reflection and transmission coefficient amplitudes for a wave in air incident upon concrete at 1 GHz calculated over a range of incidence angles for both polarizations using equations (31a) to (32b), taking the properties of concrete from Table 3.

1 Fransmission coefficient amplitude 0.9 0.9 Reflection coefficient amplitude 0.8 0.8 0.7 0.7 TE 0.6 0.6 0.5 0.5 TM0.4 0.4 TE 0.3 0.3 0.2 0.2 TM0.1 0.1 20 80 90 10 20 50 10 30 40 50 0 30 40 80 90 Angle of incidence (degrees) Angle of incidence (degrees) P.2040-02

FIGURE 2

Reflection and transmission coefficients for air/concrete interface at 1 GHz

2.2.1.3 Substitutions available in coefficient values

It can be useful to note the following substitutions for E-vector coefficients, where the subscripts denote the medium, 1 or 2, in which the wave is incident on an interface:

- a) For either polarisation, $R_1 = -R_2$, and thus $R_1^2 = R_2^2$
- b) For either polarisation, $T_1T_2 = 1 R^2$, where according to a) R can be either R_1 or R_2 .

2.2.1.4 Coefficients for power flux-densities

Coefficients for power flux densities can be obtained from the E-vector coefficients:

$$R_{STE} = \frac{S_r}{S_i} = R_{eTE}^2 \tag{34a}$$

$$R_{STM} = \frac{S_r}{S_i} = R_{eTM}^2 \tag{34b}$$

$$T_{STE} = \frac{S_t}{S_i} = T_{eTE}^2 \sqrt{\frac{\varepsilon_{rc2}}{\varepsilon_{rc1}}}$$
 (35a)

$$T_{STM} = \frac{S_t}{S_i} = T_{eTM}^2 \sqrt{\frac{\varepsilon_{rc2}}{\varepsilon_{rc1}}}$$
 (35b)

The change in signal level in decibels due to reflection or transmission is thus given by $10 \log(|R_S|)$ or $10 \log(|T_S|)$ where R_S and T_S stand for either reflection or transmission S-vector coefficient in equations (34a) to (35b).

Conservation of energy at the media interface requires that for a given incident wavefront area, the sum of the reflected and transmitted power flux equals the incident power flux. To illustrate this, account must be taken of the change in wavefront width upon refraction. For either polarization:

$$R_S + T_S \frac{\cos \theta_2}{\cos \theta_1} = 1 \tag{36}$$

where $\frac{\cos \theta_2}{\cos \theta_1}$ adjusts for the change in wavefront width.

2.2.1.5 Simplified expressions for incident wave in air

When medium 1 is air, equations (31a) to (32b) can be simplified to:

$$R_{eTE} = \frac{\cos\theta - \sqrt{\varepsilon_{rc} - \sin^2\theta}}{\cos\theta + \sqrt{\varepsilon_{rc} - \sin^2\theta}}$$
(37a)

$$R_{eTM} = \frac{\varepsilon_{rc}\cos\theta - \sqrt{\varepsilon_{rc} - \sin^2\theta}}{\varepsilon_{rc}\cos\theta + \sqrt{\varepsilon_{rc} - \sin^2\theta}}$$
(37b)

$$T_{eTE} = \frac{2\cos\theta}{\cos\theta + \sqrt{\varepsilon_{rc} - \sin^2\theta}}$$
 (38a)

$$T_{eTM} = \frac{2\sqrt{\varepsilon_{rc}}\cos\theta}{\varepsilon_{rc}\cos\theta + \sqrt{\varepsilon_{rc}-\sin^2\theta}}$$
 (38b)

where:

 θ : angle of incidence

 ε_{rc} : relative permittivity of the medium upon which the wave is incident.

Total internal reflection at the interface is not possible in equations (37a) to (38b) since it can be assumed that the wave is incident upon a medium with a higher refractive index than air.

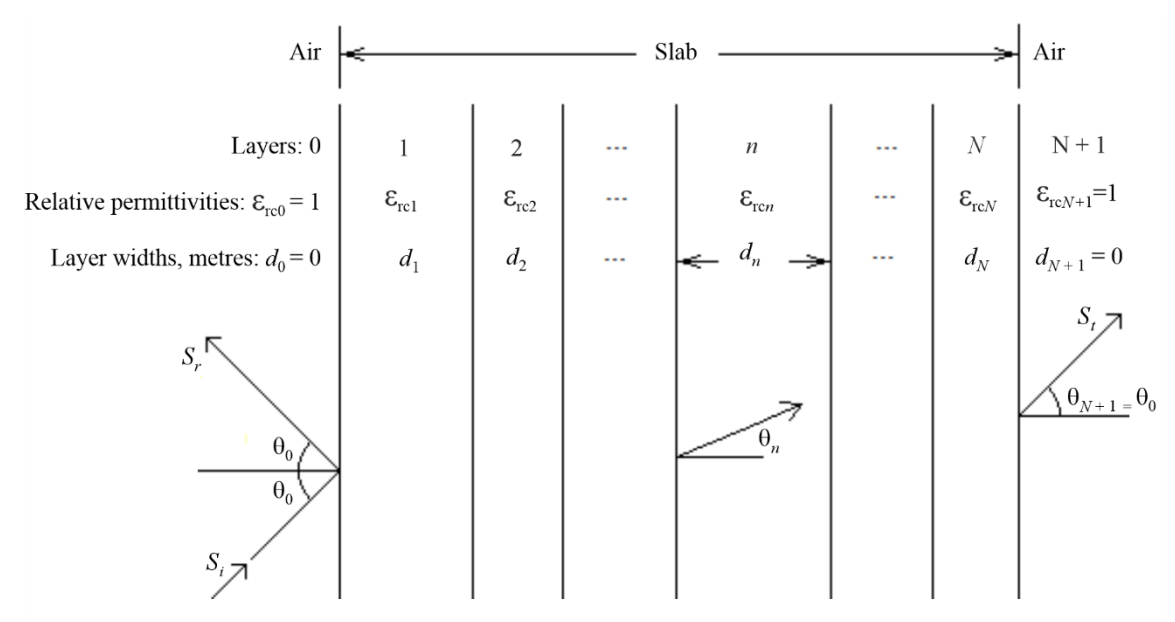
2.2.2 Plane wave reflection and transmission for a single- or multi-layer slab

2.2.2.1 General method for a multi-layer slab

Figure 3 illustrates a plane wave incident upon a slab consisting of N layers, each with smooth, planar and parallel surfaces, where N can be 1 or more. The relative permittivity of layer n is η_n , and its width d_n metres. It is assumed that the slab is in air, and for calculation purposes this is designated as layers 0 and N+1, with relative permittivity 1 and width 0.

FIGURE 3

Plane wave incident on single- or multi-layer slab



P.2040-03

The incidence and reflection angles are θ_0 , and the wave will emerge from layer N at $\theta_{N+1} = \theta_0$. The direction of propagation in layer n is θ_n . A complete ray path through the layers is not shown in Fig. 3. For a single incident ray S_i the departing rays S_r and S_t are spatially distributed due to multiple internal reflections in the layers.

Reflection coefficient for the slab can be calculated by applying equation (39) representing the reflection coefficient at the interface separating the n^{th} layer and the $(n+1)^{th}$ layer for $n=N, N-1, N-2, \ldots, 0$ with setting $R_n(N+1)=0$.

$$R_p(n) = \frac{r_p(n) + R_p(n+1) \exp(-2j\gamma_{n+1}d_{n+1})}{1 + r_p(n)R_p(n+1) \exp(-2j\gamma_{n+1}d_{n+1})}, \quad p = TE \text{ or } TM$$
(39)

In equation (39), $r_{TE}(n)$ and $r_{TM}(n)$ are the Fresnel reflection coefficient at the n^{th} interface.

$$r_{TE}(\mathbf{n}) = \frac{\sqrt{\varepsilon_{rcn}} \cos \theta_n - \sqrt{\varepsilon_{rcn+1}} \cos \theta_{n+1}}{\sqrt{\varepsilon_{rcn}} \cos \theta_n + \sqrt{\varepsilon_{rcn+1}} \cos \theta_{n+1}}$$
(40a)

$$r_{TM}(n) = \frac{\sqrt{\varepsilon_{rcn+1}} \cos \theta_n - \sqrt{\varepsilon_{rcn}} \cos \theta_{n+1}}{\sqrt{\varepsilon_{rcn+1}} \cos \theta_n + \sqrt{\varepsilon_{rcn}} \cos \theta_{n+1}}$$
(40b)

where:

$$\gamma_n = k_n \cos \theta_n = k_0 \sqrt{\varepsilon_{rcn}} \cos \theta_n = k_0 \sqrt{\varepsilon_{rcn}^2 - (\sin \theta_0)^2}$$
 (41a)

$$\sin \theta_n = \frac{\sin \theta_0}{\sqrt{\varepsilon_{rcn}}} \tag{41b}$$

$$k_n = \frac{2\pi}{\lambda} \sqrt{\varepsilon_{rcn}} \tag{41c}$$

and λ is the free-space wavelength in metres.

Having evaluated equation (39) for, in order, n = N to n = 0, the reflection coefficient R_p and the transmission coefficient T_p are given by:

$$R_p = R_p(0), p = TE, TM (42a)$$

$$T_{p} = \prod_{n=0}^{n=N} \left\{ \frac{\exp\{-j\gamma_{n}d_{n}\}\{1+r_{p}(n)\}}{\{1+r_{p}(n)R_{p}(n+1)\exp\{-2j\gamma_{n+1}d_{n+1}\}\}} \right\}, \ p = TE, TM$$
 (42b)

where the subscripts TE and TM denote transverse-electric and transverse-magnetic incident polarization respectively.

Attachment 1 to this Annex provides an alternative formulation for the multi-layer slab method.

2.2.2.2 Simplified method for a single-layer slab

For a slab consisting of a single layer, that is, for which N = 1, and the foregoing method can be simplified to:

$$R = \frac{R'(1 - \exp(-j2q))}{1 - R'^2 \exp(-j2q)} \qquad \text{(reflection coefficient)} \tag{43a}$$

$$T = \frac{(1 - R'^2)\exp(-jq)}{1 - R'^2\exp(-j2q)}$$
 (transmission coefficient) (43b)

where:

$$q = \frac{2\pi d}{\lambda} \sqrt{\varepsilon_{rc} - \sin^2 \theta} \tag{44}$$

d is the thickness of the building material, ε_{rc} is the complex relative permittivity, and R' represents R_{eTE} or R_{eTM} , as given by equations (37a) or (37b) respectively, depending on the polarization of the incident E-field.

2.2.2.3 Calculation examples

Figures 4 to 7 show examples of results from equation (42a) for a single concrete slab at 1 GHz with four incidence angles. The same results may be obtained from equations (43a) and (43b). The electrical properties for concrete are taken from Table 3.

 $FIGURE\ 4$ Reflection coefficient for a concrete slab at 1 GHz, TE polarisation

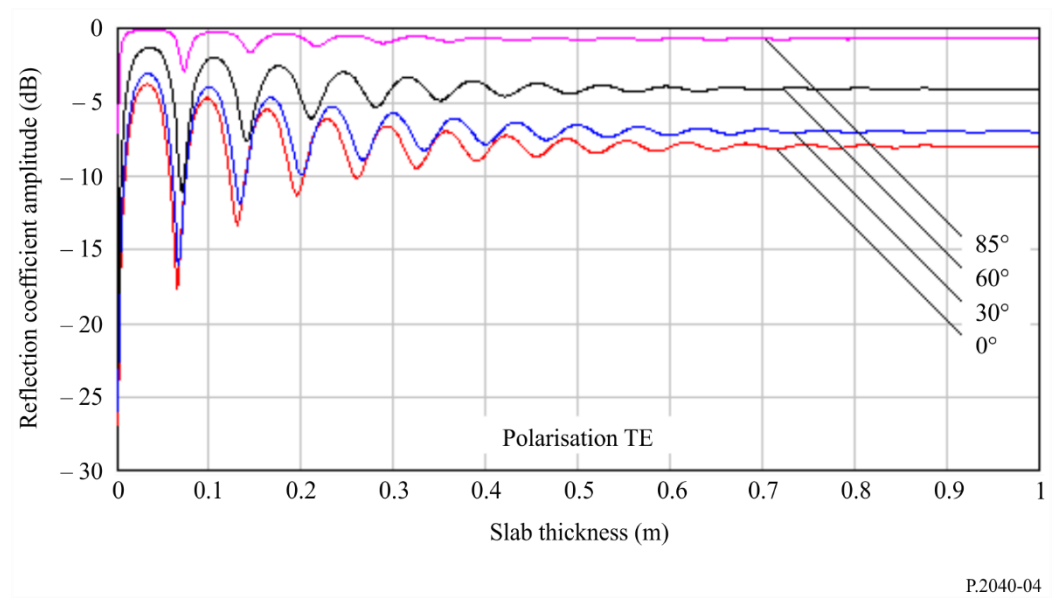
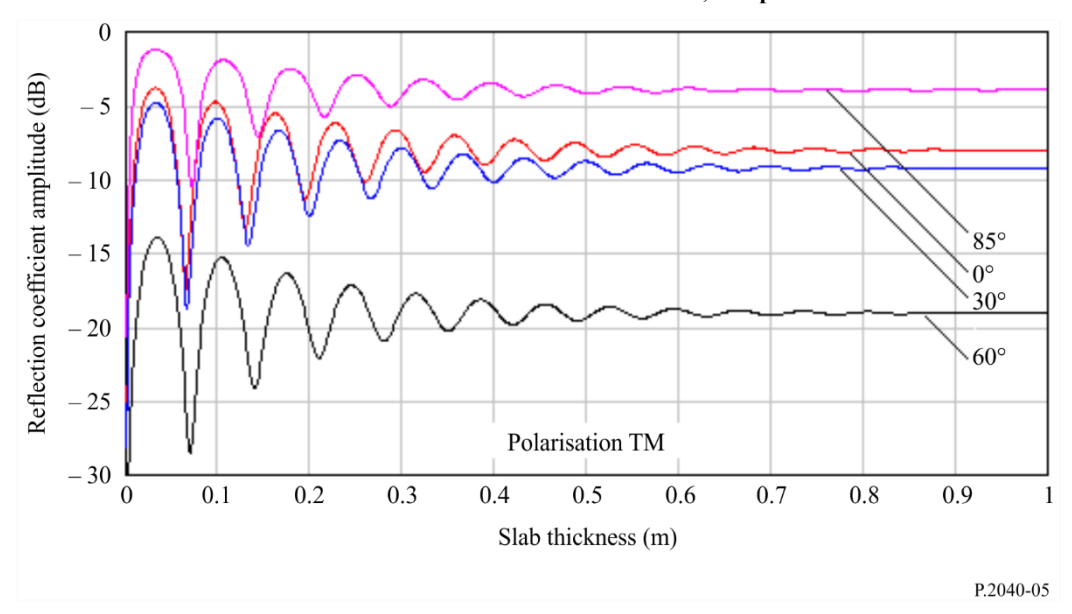
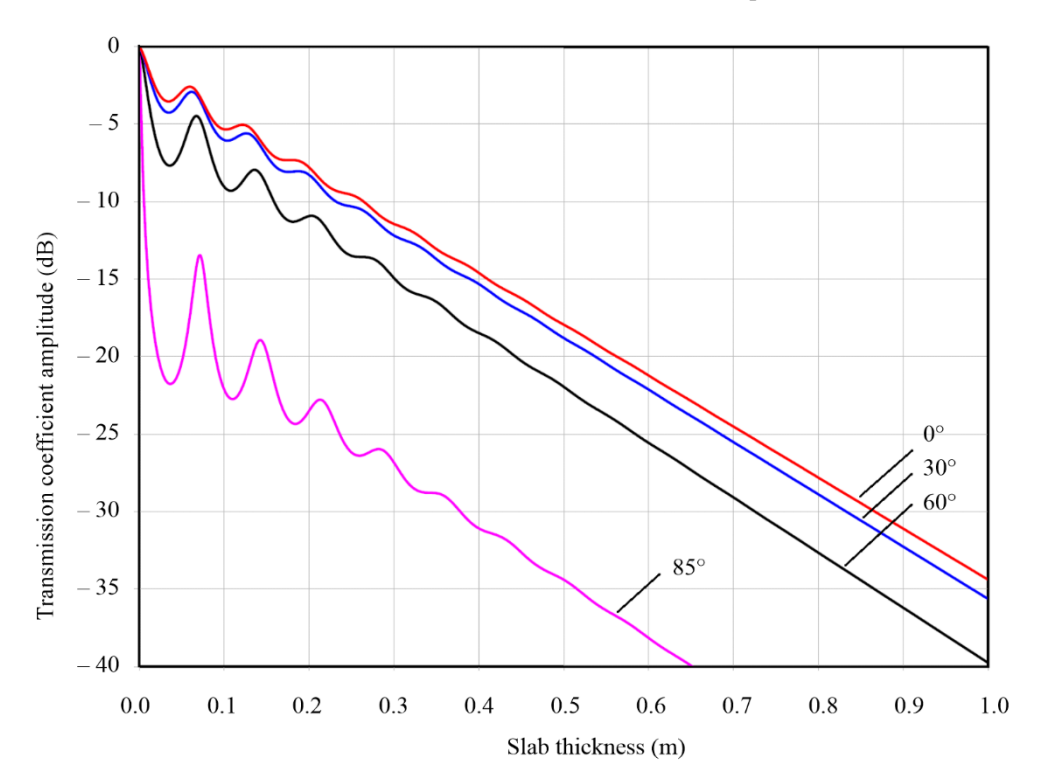


FIGURE 5
Reflection coefficient for a concrete slab at 1 GHz, TM polarisation



 $\label{eq:FIGURE 6} FIGURE~6$ Transmission coefficient for a concrete slab at 1 GHz, TE polarisation



P.2040-06

0 60° 30° -10Fransmission coefficient amplitude (dB) 85° -15-20-25309 -30-35859 -400.5 0.6 0.0 0.1 0.2 0.3 0.4 0.7 0.8 0.9 1.0 Slab thickness (m) P.2040-07

FIGURE 7

Transmission coefficient for a concrete slab at 1 GHz, TM polarisation

1.2010 07

It will be noted in Figs 5 and 7 that the coefficients for TM polarization for 85 degrees incidence have anomalous values compared to the ordering of the other three angles. This is the effect of the minimum in reflection coefficient visible in Fig. 2 for TM polarization, known as the pseudo-Brewster angle.

2.2.3 Waveguide propagation in buildings

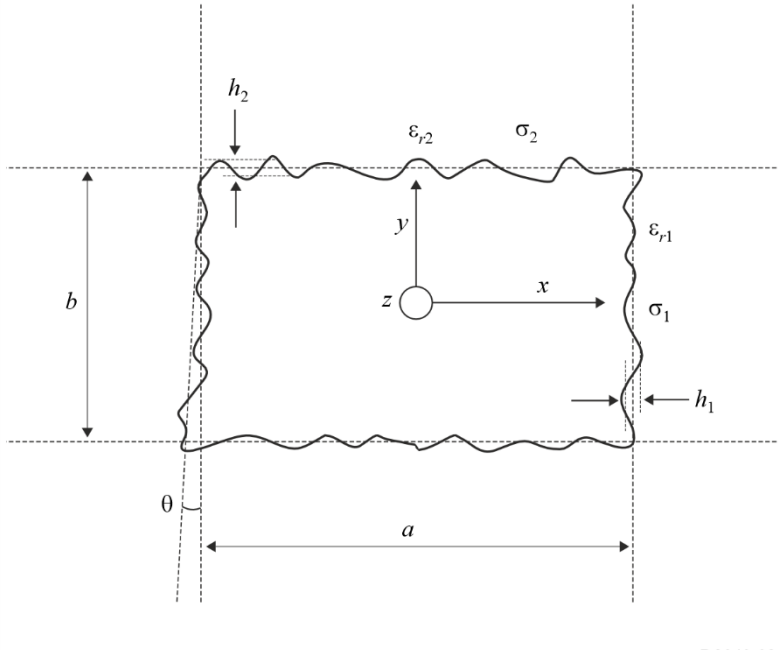
2.2.3.1 Theory on frequency characteristics of attenuation constant in waveguide

A waveguide may comprise of a hollow space surrounded by lossy dielectric materials. In the case of a building structure, a corridor, underground mall, or tunnel can be considered as a waveguide. The radio-wave power that propagates in a waveguide is attenuated according to the distance. It is well known that a waveguide has frequency characteristics such as the cut-off frequency that varies according to the shape. In this section, a formula is presented to derive the attenuation constant for the frequency characteristics in a waveguide.

The cross-section of a square waveguide structure is shown in Fig. 8. In this case, the intrinsic constants of the lossy dielectric material are different for the sidewalls and for the ceiling and the floor.

FIGURE 8

Cross-section of waveguide and material constants



P.2040-08

In Fig. 8, a is the width and b is the height of the waveguide (m), h_1 and h_2 are the root mean square roughness of the Gaussian distribution of the surface level, and θ is the tilt of the root mean square (rad). The complex permittivity values for materials ε_{ri}^* are calculated as follows.

$$\varepsilon_{ri}^* = \varepsilon_{ri} - j \left(\varepsilon_{ri}^" + \frac{\sigma_i}{\varpi \varepsilon_0} \right), \quad i = 1,2$$
(45)

where ε_{ri} is the relative dielectric constant and σ_i is the conductivity. The quantity ε_{ri} " is the loss tangent of the materials, ω is the angular frequency and ε_0 is the permittivity of free space.

The basic attenuation constant is formulated as follows.

$$L_{basic,h} = K_{h} \lambda^{2} \left[Re \left(\frac{\varepsilon_{r1}^{*}}{a^{3} \sqrt{\varepsilon_{r1}^{*} - 1}} + \frac{1}{b^{3} \sqrt{\varepsilon_{r2}^{*} - 1}} \right) - \frac{\lambda}{2\pi} Im \left(\frac{\left|\varepsilon_{r1}^{*}\right|^{2}}{a^{4} \left(\varepsilon_{r1}^{*} - 1\right)} + \frac{1}{b^{4} \left(\varepsilon_{r2}^{*} - 1\right)} \right) \right]$$

$$L_{basic,v} = K_{v} \lambda^{2} \left[Re \left(\frac{1}{a^{3} \sqrt{\varepsilon_{r1}^{*} - 1}} + \frac{\varepsilon_{r2}^{*}}{b^{3} \sqrt{\varepsilon_{r2}^{*} - 1}} \right) - \frac{\lambda}{2\pi} Im \left(\frac{1}{a^{4} \left(\varepsilon_{r1}^{*} - 1\right)} + \frac{\left|\varepsilon_{r2}^{*}\right|^{2}}{b^{4} \left(\varepsilon_{r2}^{*} - 1\right)} \right) \right]$$

$$(46)$$

 K_h and K_v are constant values that are dependent on the section shape. The constant values dependent on the section shape are given in Table 1.

TABLE 1

Constant values for various cross-section shapes

Shape	Circle	Ellipse	Square	Arch-backed
K_h	5.09	4.45	4.34	5.13
$K_{\rm v}$	5.09	4.40	4.34	5.09

The formulas mentioned above are valid based on equation (47) representing the condition of constraint.

$$\lambda \ll \frac{\pi a \sqrt{\varepsilon_{r_1} - 1}}{\varepsilon_{r_1}}$$

$$\lambda \ll \pi b \sqrt{\varepsilon_{r_2} - 1}$$
(m)
(47)

Unique characteristics in square shape case

The attenuation constant due to roughness, which is regarded as local variations in the level of the surface relative to the mean level of the surface of a wall, is given by:

$$L_{roughness,h} = K_{h} \pi^{2} \lambda \left[\left(\frac{h_{1}}{a^{2}} \right)^{2} + \left(\frac{h_{2}}{b^{2}} \right)^{2} \right]$$

$$L_{roughness,v} = K_{v} \pi^{2} \lambda \left[\left(\frac{h_{1}}{a^{2}} \right)^{2} + \left(\frac{h_{2}}{b^{2}} \right)^{2} \right]$$

$$(48)$$

The attenuation constant due to the wall tilt is given by:

$$L_{tilt,h} = K_{h} \frac{\pi^{2} \theta^{2}}{\lambda}$$

$$L_{tilt,v} = K_{v} \frac{\pi^{2} \theta^{2}}{\lambda}$$
(dB/m)
(49)

Therefore, the total attenuation constant in a square shape case is the sum of the above losses:

$$L_h = L_{basic,h} + L_{roughness,h} + L_{tilt,h}$$

$$L_v = L_{basic,v} + L_{roughness,v} + L_{tilt,v}$$
(50)

2.2.3.2 Applicability of waveguide theory

The waveguide theory shows good agreement with the measured propagation characteristics in the corridor in the frequency range of 200 MHz to 12 GHz in case there is no pedestrian traffic in the corridor.

Effect of pedestrian traffic on waveguide

Figure 9 shows a comparison of the theoretical and measured attenuation constant values during the day (when pedestrian traffic is present), and during the night (when the corridor is empty). Theoretical values are calculated based on the parameters given in Table 2.

TABLE 2

Parameters used in underground calculation

	Width	Height	Tilt	Roug	ghness	N	Material	constan	ıt
	(m)	(m)	(degrees)	h_1	h_2	€ _{r1}	ε_{r2}	σ_1	σ_2
Underground	6.4	3.0	0.35	0.4	0.2	15	10	0.5	0.1

FIGURE 9

Attenuation constant comparison for day and night

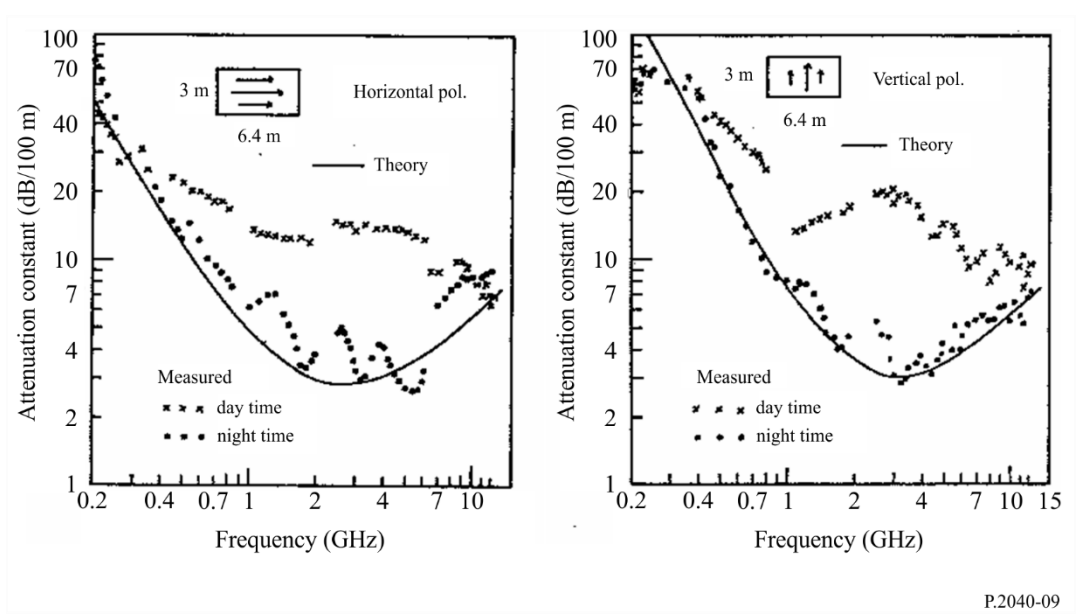


Figure 9 shows that the waveguide theory is applicable to realistic propagation characteristics in the corridor in the frequency range of 200 MHz to 12 GHz at night. However, the waveguide theory is not applicable to realistic propagation characteristics during daytime, because the received power is attenuated by pedestrian traffic.

Therefore, the waveguide theory is applicable to situations where there is no influence from shadowing obstacles.

2.3 Theory and results for frequency selective surface materials

2.3.1 Frequency selective surfaces

The power of scattering waves varies with roughness of surfaces. In this section, a theory for calculating scattered fields from the surface having round convexity array is described. First, for parameterizing the roughness of the surface, the rough surface is defined by using a round convexity array formed by locating circular cylinders periodically.

Second, the reflection coefficient of the scattered fields is defined by using the lattice sums characterizing a periodic arrangement of scatterers and the T-matrix for a circular cylinder array. Third, a numerical result that shows the frequency-depending characteristic of the reflection from the round convexity's surface is shown. Finally, a measurement result is shown to explain that the power of scattering waves varies with the frequency of an incident wave when there is a round convexity array on the surface of a building.

2.3.2 Theory for wave propagation around the surface of round convexity array

By making periodical round convexity array on a surface of a building, as shown in Fig. 10, reflection/scattering waves can be controlled larger than those from the flat surface. The theory to calculate the scattered waves from the periodic arrays of circular cylinders can be used to define the propagation waves around a convexity array of a surface.

FIGURE 10

The surface of round convexity array

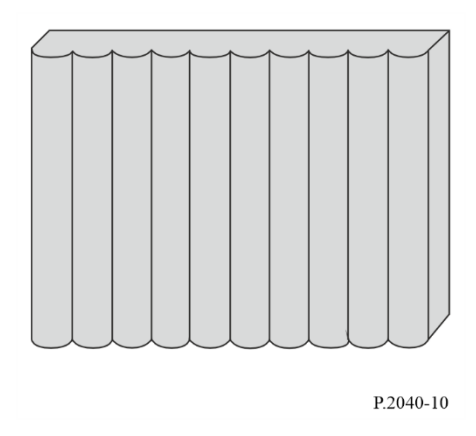
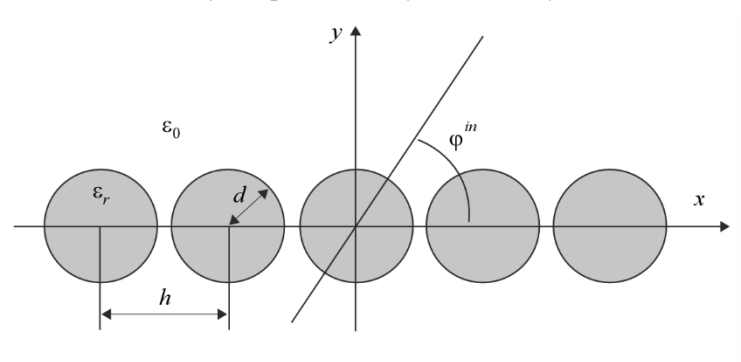


FIGURE 11

Geometry of a periodic array of circular cylinders



When the identical circular cylinders are situated periodically in an x axis as shown in Fig. 11, the power reflection coefficient R_v for the v-th propagating mode with $k_v > 0$ is given as:

$$R_{\nu} = \frac{k_{\nu}}{k_{0} \sin \omega^{\text{in}}} |\boldsymbol{p}_{\nu}^{T} \cdot \boldsymbol{a}_{0}^{\text{sc}}|^{2}$$

$$\tag{51}$$

P.2040-11

where $k_0 = 2\pi / \lambda_0$, λ_0 is the wavelength of the waves indenting in angle φ^{in} . In equation (51), \boldsymbol{p}_{ν}^T and \boldsymbol{a}_0^{sc} are obtained as follows:

$$\boldsymbol{p}_{\nu} = \begin{bmatrix} \frac{2(j)^{m}(k_{x\nu} + jk_{\nu})^{m}}{hk_{\nu}k_{0}^{m}} & (m \ge 0) \\ \frac{2(-j)^{|m|}(k_{x\nu} - jk_{\nu})^{|m|}}{hk_{\nu}k_{0}^{|m|}} & (m < 0) \end{bmatrix}$$
(52)

$$\boldsymbol{a}_0^{\text{sc}} = (\overline{\boldsymbol{I}} - \overline{\boldsymbol{T}} \cdot \overline{\boldsymbol{L}})^{-1} \cdot \overline{\boldsymbol{T}} \cdot \boldsymbol{a}^{in}$$
 (53)

where \bar{I} is the unit matrix, $k_{xv} = -k_0 \cos \varphi^{in} + \frac{2v\pi}{h}$, $k_v = \sqrt{k_0^2 - k_{xv}^2}$ and h is the periodic space between each round convex. \bar{L} is a square matrix whose elements are defined in terms of the following lattice sums:

$$L_{mn} = \sum_{l=0}^{\infty} H_{m-n}^{(1)}(k_0 l h) e^{jk_0 l h \phi^{in}} + (-1)^{m-n} \sum_{l=0}^{\infty} H_{m-n}^{(1)}(k_0 l h) e^{-jk_0 l h \phi^{in}}$$
(54)

where $H_m^{(2)}$ is the *m*-th order Hankel function of the first kind. \overline{T} is the T-matrix for the scattered fields and is given by the following diagonal matrix for the incident electric field E_z^{in} and the incident magnetic field H_z^{in} , respectively.

$$T_{mn}^{E} = -\frac{\sqrt{\varepsilon_{r}}J'_{m}(kd)J_{m}(k_{0}d) - J_{m}(kd)J'_{m}(k_{0}d)}{\sqrt{\varepsilon_{r}}J'_{m}(kd)H_{m}^{(1)}(k_{0}d) - J_{m}(kd)H_{m}^{'(1)}(k_{0}d)}\delta_{mn}$$
(55a)

$$T_{mn}^{H} = -\frac{J_{m}'(kd)J_{m}(k_{0}d) - \sqrt{\varepsilon_{r}}J_{m}(kd)J_{m}'(k_{0}d)}{J_{m}'(k_{0}d)H_{m}^{(1)}(k_{0}d) - \sqrt{\varepsilon_{r}}J_{m}(kd)H_{m}'^{(1)}(k_{0}d)}\delta_{mn}$$
(55b)

where ε_r is the relative permittivity of the dielectric cylinder, J_m is the *m*-th order Bessel function, the prime demotes the derivative with respect to the argument, and δ_{mn} denotes the Kronecker's delta. a^{in} denotes a column vector whose elements represent unknown amplitudes of the incident field.

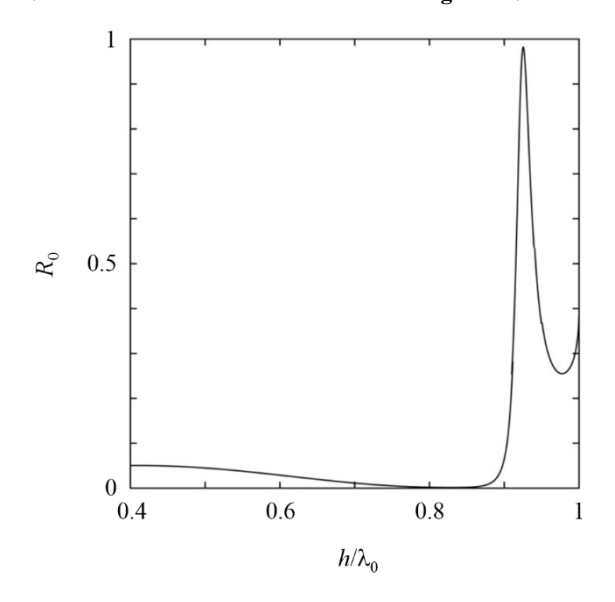
$$\boldsymbol{a}^{in} = \left[(j)^n e^{-jn\varphi^{in}} \right] \tag{56}$$

2.3.3 Calculation results

The calculation result of a power reflection coefficient is shown in Fig. 12. The result is calculated by using equation (51) in the case that the electric field E_z^{in} is transmitted in the angle $\varphi^{in} = 90^\circ$ to the dielectric round convexities whose diameter and permittivity are d = 0.3h and $\varepsilon_r = 2.0$, respectively. In the result, there is the frequency band that the incident wave is reflected almost completely by the surface even if its material is a lossless dielectric substance.

FIGURE 12

Power reflection coefficient R_0 as functions of the normalized wavelength h/λ_0 at normal incidence electric field E_z^{in}



P.2040-12

2.3.4 Measurement

The measurements of the scattered waves from the building having the round convexity array were carried out. Figure 13 shows the comparison of the scattered waves from the building between the flat surface and the surface with round convexity arrays. The scattered waves from the building were measured in various reflected angles φ^r between 30° to 90°, when the electric field is transmitted in the angle φ^m . The incident angle and reflection angle are defined as shown in Fig. 14.

FIGURE 13

Geometry of a periodic array of circular cylinders

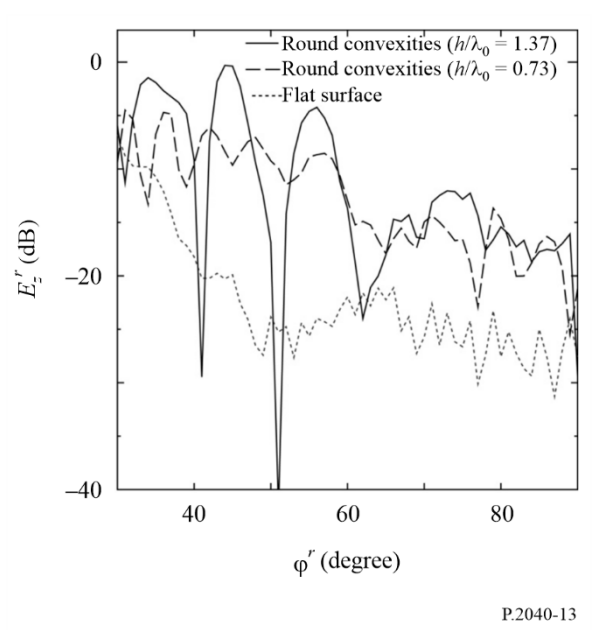
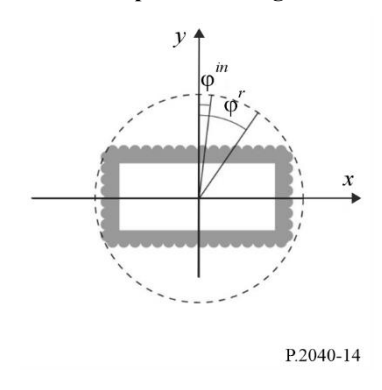


FIGURE 14

A plane figure of the compositional diagram for measurements



The measurement results show that the power of the scattered field from the surface having a round convexity array becomes larger than that from the flat surface, and can be controlled by the period between and diameter of each round convexity. Note that the relative permittivity and the conductivity of the building material were estimated as $\varepsilon_r = 6.0$ and $\sigma = 0.1$ S/m, respectively.

3 Compilations of electrical properties of materials

Representative data on material electrical properties can be hard to find, as characteristics are expressed using different combination of parameters, and the relative permittivity may be quoted at

frequencies that are not close to that of interest. A table of representative material properties has therefore been compiled using the curve-fitting approach described in § 2.1.4.

Data from eight sets of material electrical properties (a total of more than 90 separate characteristics) given in the open literature have been collated, converted to a standard format and grouped into material categories.

For each group, simple expressions for the frequency-dependent values of the real part of the relative permittivity, ε'_r , and the conductivity, σ , were derived. These are:

$$\varepsilon_r' = af^b \tag{57}$$

and:

$$\sigma = cf^d \tag{58}$$

where f is frequency in GHz and σ is in S/m. (ε'_r is dimensionless.) The values of a, b, c and d are given in Table 3. Where the value of b or d is zero the corresponding value of ε'_r or σ is a or c respectively, and independent of frequency.

If required, the imaginary part of the relative permittivity ε_r'' can be obtained from the conductivity and frequency:

$$\varepsilon'' = \frac{17.98\sigma}{f} \tag{59}$$

Parameters for air, metal and three conditions of ground are included in Table 3 for completeness.

TABLE 3

Examples of material properties¹

Material class	rial class Real part of relative permittivity Conductive S/m		•	Frequency range (GHz)	
	а	b	С	d	
Vacuum (≈ air)	1	0	0	0	0.001-100
Concrete	5.24	0	0.0462	0.7822	1-100
Concrete	5.17	0	0.0145	1.0900	110-330
Brick	3.91	0	0.0238	0.16	1-40
Brick	4.15	0	0.0006	1.5712	110-330
Plasterboard	2.73	0	0.0085	0.9395	1-100
Plasterboard	2.56	0	0.0001	1.7799	110-330
Plasterboard	2.65	0	0.0002	1.598	100-400
Wood	1.99	0	0.0047	1.0718	0.001-100
Wood	1.82	0	0.0040	1.0761	110-330

¹ Examples of measured electrical characteristics of different materials that could be in the same material class.

TABLE 3 (end)

Material class		of relative ttivity	Conduc S/i	•	Frequency range (GHz)	
Wood	2.1183	0	0.0055 1.1113		100-400	
Glass	6.31	0	0.0036	1.3394	0.1-100	
Glass	5.79	0	0.0004	1.658	220-450	
Glass	6.5767	0	0.0012	1.4697	100-400	
Clear Acrylic	2.58	0	0.0001	1.6524	110-330	
Ceiling board	1.48	0	0.0011	1.0750	1-100	
Ceiling board	1.52	0	0.0029	1.029	220-450	
Ceiling board	1.2567	0	0.00013	1.454	100-400	
Chipboard	2.58	0	0.0217	0.7800	1-100	
Chipboard	2.16	0	0.0023	1.359	100-200	
Plywood	2.71	0	0.33	0	1-40	
Plywood	1.94	0	0.0067	0.9982	110-330	
Plywood	2.17	0	0.0063	1.045	100-400	
Marble	7.074	0	0.0055	0.9262	1-60	
Marble	7.94	0	0.0001	1.7330	110-330	
Marble	8.62	0	0.0027	1.15	100-400	
Floorboard	3.66	0	0.0044	1.3515	50-100	
Floorboard	5.27	0	2.22×10 ⁻¹⁷	7.3413	220 ≤ f < 300	
Floorboard	5.27	0	0.0003	2.0298	300 ≤ <i>f</i> < 400	
Floorboard	5.27	0	49.8726	0	400 ≤ <i>f</i> < 450	
Floorboard	3.1575	0	0.001675	1.32775	100-400	
Vinyl tile	3.62	0	0.0051	0.8422	1-40	
Carpet tile	2.08	0	0.0009	0.8200	1-40	
Asphalt concrete	4.83	0	0.0108	1.3969	1-40	
Metal	1	0	107	0	1-100	
Very dry ground	3	0	0.00015	2.52	1-10 only	
Medium dry ground	15	-0.1	0.035	1.63	1-10 only	
Wet ground	30	-0.4	0.15	1.30	1-10 only	

The frequency ranges given in Table 3 are not hard limits but are indicative of the measurements used to derive the models. The exceptions are the three ground types where the 1-10 GHz frequency limits must not be exceeded. Typical values of relative permittivity and conductivity for different types of ground, as function of frequency in the range 0.01 MHz to 100 GHz, are given in Recommendation ITU-R P.527.

The loss tangents of all the dielectric materials in Table 3 are less than 0.5 over the frequency ranges specified. The dielectric limit approximations for the attenuation rate given in equations (24) and (27) can therefore be used to estimate the attenuation of an electromagnetic wave through the materials.

Attachment 1 to Annex 1

Alternative method to obtain reflection and transmission coefficients for building materials represented by N dielectric slabs based on ABCD matrix formulation

An alternative formulation of the method in § 2.2.2.1 is given below to obtain the reflection, R, and transmission, T, coefficients for a building material represented by N dielectric slabs based on the ABCD matrix formulation, as illustrated in Fig. 5. The regions on both sides of the building material are assumed to be free space. This alternative method produces exactly the same results as that given in § 2.2.2.1.

$$R = \frac{B/Z_0 - CZ_0}{2A + \frac{B}{Z_0} + CZ_0} \tag{60a}$$

$$T = \frac{2}{2A + \frac{B}{Z_0} + CZ_0} \tag{60b}$$

where A, B and C are the elements of the ABCD matrix given, using matrix multiplication, by:

$$\begin{bmatrix} A & B \\ C & D \end{bmatrix} = \begin{bmatrix} A_1 & B_1 \\ C_1 & D_1 \end{bmatrix} ... \begin{bmatrix} A_m & B_m \\ C_m & D_m \end{bmatrix} ... \begin{bmatrix} A_N & B_N \\ C_N & D_N \end{bmatrix}$$
(61a)

where:

$$A_m = \cos(\beta_m d_m) \tag{61b}$$

$$B_m = jZ_m \sin(\beta_m d_m) \tag{61c}$$

$$C_m = \frac{j\sin(\beta_m d_m)}{Z_m} \tag{61d}$$

$$D_m = A_m (61e)$$

$$\beta_m = k_m \cos(\theta_m) = k_m \left[1 - \frac{\sin^2 \theta_0}{\varepsilon_{rcm}} \right]^{\frac{1}{2}}$$
 (61f)

$$k_0 = \frac{2\pi}{\lambda} \tag{61g}$$

$$k_m = k_0 \sqrt{\varepsilon_{rcm}} \tag{61h}$$

where:

 λ : free-space wavelength

 k_0 : free-space wave number

 $\varepsilon_{\rm rcm}$: complex relative permittivity in the *m*-th slab

 k_m : wave number in the m-th slab

 β_m : propagation constant in the direction perpendicular to the slab plane

 d_m : width of the m-th slab.

The wave impedances Z are given, according to incidence polarization, by:

$$Z_m = \frac{120\pi}{\sqrt{\varepsilon_{rcm}\cos\theta_m}}$$
 TE polarisation (62a)

$$Z_m = \frac{120\pi\cos\theta_m}{\sqrt{\varepsilon_{rcm}}}$$
 TM polarisation (62b)

where:

$$\varepsilon_{rc0} = \varepsilon_{rcN+1} = 1 \tag{63a}$$

$$\Theta_0 = \theta_{N+1} = \theta \tag{63b}$$

$$Z_0 = Z_{N+1} \tag{63c}$$

The wave impedance Z_0 in equation (63c) is the free space impedance, and it can be obtained from equations (62a) and (62b) through setting $\varepsilon_{rcm} = 1$.